MedChemComm

Accepted Manuscript

This article can be cited before page numbers have been issued, to do this please use: K. Kucwaj-Brysz, R. Kurczab, E. esawska, A. Lubelska, M. A. Mar, G. Latacz, G. Sataa, W. Nitek, K. Kononowicz and J. Handzlik, *Med. Chem. Commun.*, 2018, DOI: 10.1039/C8MD00168E.

ROYAL SOCIETY OF CHEMISTRY

rsc.li/medchemcomm

View Article Online
DOI: 10.1039/C8MD00168E

The role of aryl-topology for balancing between selective and dual 5-HT$_7$R/5-HT$_{1A}$ action of 3,5-substituted hydantoins

Katarzyna Kucwaj-Brysz[1], Rafał Kurczab[2], Ewa Żesławska[3], Annamaria Lubelska[1], Małgorzata Anna Marć[1], Gniewomir Latacz[1], Grzegorz Satała[2], Wojciech Nitek[4], Katarzyna Kieć-Kononowicz[1], Jadwiga Handzlik[1,*]

[1] *Department of Technology and Biotechnology of Drugs, Jagiellonian University Medical College, Medyczna 9, 30-688 Cracow, Poland*
[2] *Department of Medicinal Chemistry Institute of Pharmacology, Polish Academy of Science, Smętna 12, 31-343, Cracow, Poland*
[3] *Department of Chemistry, Institute of Biology, Pedagogical University of Cracow, Podchorążych 2, 30-084 Cracow, Poland*
[4] *Faculty of Chemistry, Jagiellonian University, Gronostajowa 2, 30-387, Cracow, Poland*
* *Correspondence: jhandzli@cm-uj.krakow.pl; Tel.: +012 620 55 80*

Abstract:

In order to search for active and selective serotonin 5-HT$_7$R antagonists among 3,5-disubstituted arylpiperazine-imidazolidine-2,4-diones, the role of introduction/deletion and mutual orientation of aromatic rings was analyzed. Chemical modifications of 2nd generation lead structure, 3-(3-(4-(diphenylmethyl)piperazin-1-yl)-2-hydroxypropyl)-5-(4-fluorophenyl)-5-methylimidazolidine-2,4-dione (**2**, KKB16) were performed. New derivatives (**4**-**18**) were designed and synthesized. The X-ray crystallographic analysis for representative compound, 5-(4-fluorophenyl)-3-[2-hydroxy-3-(4-phenylpiperazin-1-yl)propyl]-5-methylimidazolidine-2,4-dione (**3**), was performed to support molecular modeling and SAR studies. The affinity for 5-HT$_7$R, D$_2$R and 5-HT$_{1A}$R in the radioligand binding assays for whole series and ADME-Tox parameters *in vitro* for selected compounds (**7**, **10**, **13**), were evaluated. The molecular docking and pharmacophore model assessment were performed. As results, 5-methyl-5-naphtylhydantoin derivatives were found as new highly active 5-HT$_7$R agents (K_i ≤ 5 nM) with significant selectivity over 5-HT$_{1A}$R and D$_2$R. In contrary, the (1-naphthyl)piperazine moiety gained with the potent dual 5-HT$_7$R/5-HT$_{1A}$R action (K_i: 11 nM/19 nM).

Introduction

Targeting receptor 5-HT$_7$, the youngest member of serotoninergic system[1–3] , seems to be a promising approach in terms of treatment of CNS disorders such as depression[4] and schizophrenia-like cognitive impairments[5]. However considering design of 5-HT$_7$R ligands, the same dilemma still remains if selective[6,7] or rather multitargeted therapy[8,9] is better solution for the CNS patients. The selective mechanism of action, targeting only into the desired protein, gives hope for decrease probability of side-effects manifestation, caused by interactions with off-targets. Going deeper according to functional selectivity approach, it is

View Article Online
DOI: 10.1039/C8MD00168E

possible to activate not only chosen biological target, but specific signal transduction pathway[6]. It is also worth mentioning that only one selective 5-HT_7R ligand, compound JNJ-18038683, has been studied in clinical trials, but unfortunately its antidepressant action has not been proved due to the lack of sensitivity of performed studies[7]. Thus, searching for a potent and selective 5-HT_7R ligands seems to be significant direction in order to verify potential advantages and disadvantages of selective therapy.

In contrary, polypharmacology is suggested to be an appropriate solution for an achievement of high efficacy of complex therapy, e.g. of mood disorders and schizophrenia[8,9] or of both, cancer and CNS diseases[10]. Some trends in search for so called « magic shotguns » against most common central nervous system disorders[11] indicate an importance of serotonin and dopamine targets, apart from 5-HT_7, also 5-HT_{1A}[8] and D_2[9] receptors. However, lines of evidence demonstrate various dual- and multitarget acting compounds useful against CNS-disorders, which involve serotoninergic and other GPCRs, e.g. muscarinic M_4 receptors against schizophrenia[12] or "non-monoaminergic" mechanisms, e.g. neurokinin NK_1 antagonists against depression[13]. To the date, 5-HT_7R antagonists, acting in multidirect way, are available on pharmaceutical market, e.g. vortioxetine, approved in 2013 by FDA for treatment of major depressive disorder[14,15] or lurasidon, the second generation antipsychotic drug[16].

Our previous studies led to synthesis of 30-membered group of hydantoin-derived 5-HT_7 ligands[17–19]. Nineteen of them are highly active (K_i < 100 nM) and selective over other GPCR's (5-HT_{1A}, D_2, 5-HT_7, α_{1A}-, α_{2B}-, β_2-adrenoceptors). Behavioral studies (Porsolt's test), performed for selected compounds, confirmed their antidepressant activitiy in mice. Worth noting, that not the 1st generation lead (MF-8, **1**, Fig. 1) with the strongest affinity towards 5-HT_7[18,20] but the lead derivative (KKB16, **2**, Fig. 1) with the highest metabolic stability turned up to cause the most significant antidepressant effect[21]. Moreover, the compound **2** showed also the highest selectivity over 5-HT_{1A}R (71-fold) within the whole series. According to SAR analysis including **2** in comparison to majority of derivatives with (un)substituted phenyl ring[18,19], the observed selectivity seemed to be a consequence of presence of diphenylmethyl group linked to piperazine.

View Article Online
DOI: 10.1039/C8MD00168E

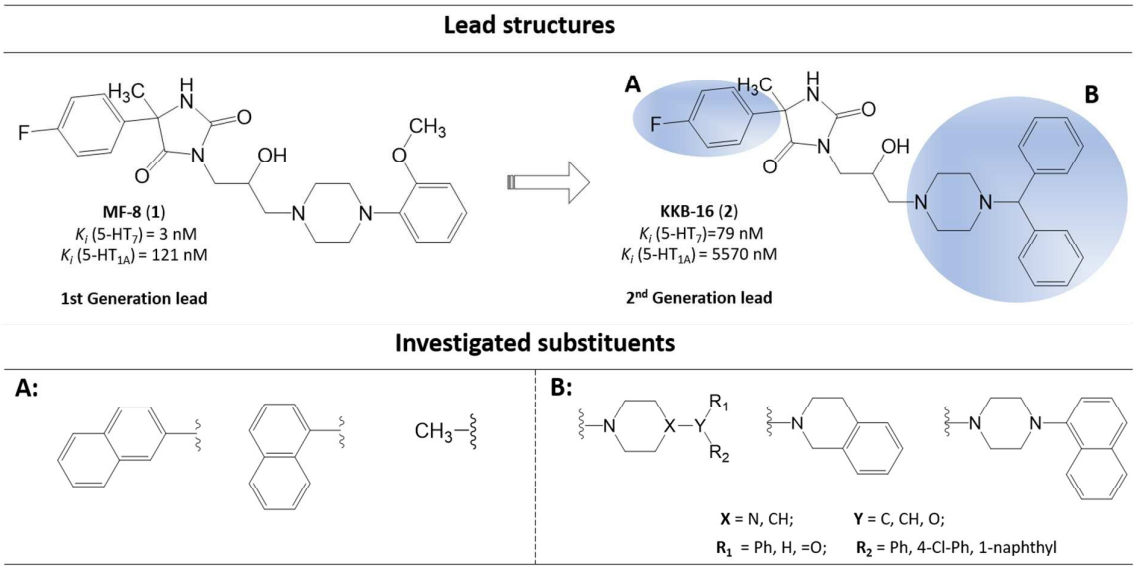

Fig. 1. Lead structures (MF-8, KKB-16) and areas of their modifications explored within this work.

Hence, the aforementioned issues are worth to be further studied in order to verify (i) how changes in number and (mutual) spatial orientation of aromatic rings influence activity and selectivity for 5-HT$_7$R among the hydantoin-derived ligands and (ii) the importance of diphenylmethyl group for beneficial metabolic stability. For this purpose, the diphenylmethyl derivative (**2**) was selected as the 2nd generation lead structure to be modified within « antipodal » aromatic-containing areas (blue, Fig. 1). Both generations leads, **1** and **2,** and the previously investigated 5-phenyl derivative **3**[18] (Table 1) were used as reference compounds for these studies. Fifteen novel derivatives of lead **2** were designed and synthesized (**4**-**18**, Table 1). The new compounds were tested in the radioligand binding assay in order to assess affinity towards 5-HT$_7$R, 5-HT$_{1A}$ and D$_2$. X-ray crystallographic analysis of **3** was performed. To elucidate differences in the 5-HT$_7$R activity and selectivity, molecular modeling, docking- and pharmacophore-based, studies were performed. Selected compounds (**7**, **10** and **13)** were examined on their metabolic stability and toxicity *in vitro* in comparison to both leads (**1** and **2**).

View Article Online
DOI: 10.1039/C8MD00168E

Table 1. Structures and radioligand binding results for compounds **1-18**.

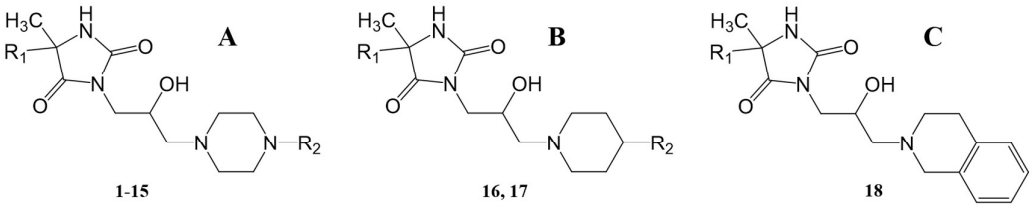

Cpd	Group	R^1	R^2	K_i [nM]		
				D_2R^1	5-$HT_{1A}R^2$	5-HT_7R^3
1*	A	4-Fluorophenyl	2-MeO-phenyl	715	121	3
2*	A	4-Fluorophenyl	Diphenylmethyl	261	5570	79
3*	A	4-Fluorophenyl	Phenyl	2906	2733	223
4	A	4-Fluorophenyl	Benzyl	20030	377500	2085
5	A	4-Fluorophenyl	Benzoyl	10080	6216	3609
6	A	4-Fluorophenyl	(Naphthalene-1-yl)methyl	5233	5577	2172
7	A	4-Fluorophenyl	1-Naphthyl	295	19	11
8	B	4-Fluorophenyl	Phenoxyl	4353	5211	165
9	B	4-Fluorophenyl	4-Cl-Phenoxyl	4116	21470	172
10	A	1-Naphthyl	2-MeO-Phenyl	256	326	5
11	A	1-Naphthyl	2-CN-Phenyl	416	1225	19
12	A	1-Naphthyl	Diphenylmethyl	273	413200	224
13	A	2-Naphthyl	2-MeO-Phenyl	153	128	3
14	A	2-Naphthyl	2-CN-Phenyl	264	129	3
15	A	Methyl	2-MeO-Phenyl	2130	489	125
16	A	Methyl	2-CN-Phenyl	3429	1155	209
17	A	Methyl	Diphenylmethyl	1152	15150	824
18	C	4-Fluorophenyl	-	5848	1551	888
Ref[a-c]				9[a]	20[b]	18[c]

*Compounds from the previously published and pharmacologically described series.[1-3] Radioligands used: [^{3}H]-Raclopride (D_2R), [^{3}H]-8-OH-DPAT (5-$HT_{1A}R$), [^{3}H]-5-CT (5-HT_7R). [a-c]Reference ligands for GPCRs investigated: [a]olanzapine, [b]buspirone, [c]clozapine, nt - not tested.

Results and discussion

Synthesis

The designed new derivatives (**4–18**) were obtained based on previously optimized three-step pathway[19] starting from Bucherer-Bergs reaction, which led to hydantoin system

View Article Online
DOI: 10.1039/C8MD00168E

formation, followed by N-alkylation with epichlorhydrin and solvent-free microwave-assisted condensation with simultaneous epoxide opening at the end (Scheme 1). Compounds **15–17** were synthesized in two steps, starting from commercially available 5,5-dimethylhydantoin. Pure products have been isolated during pH-dependent extraction. This method allowed to eliminate time- and cost-consuming purufication by column chromatography used previously[18,19]. All the compounds were obtained as racemic mixtures due to non-stereoselectivity of Bucher-Bergs reaction and application of (+/-)-2-(chloromethyl)oxirane as alkylating agent.

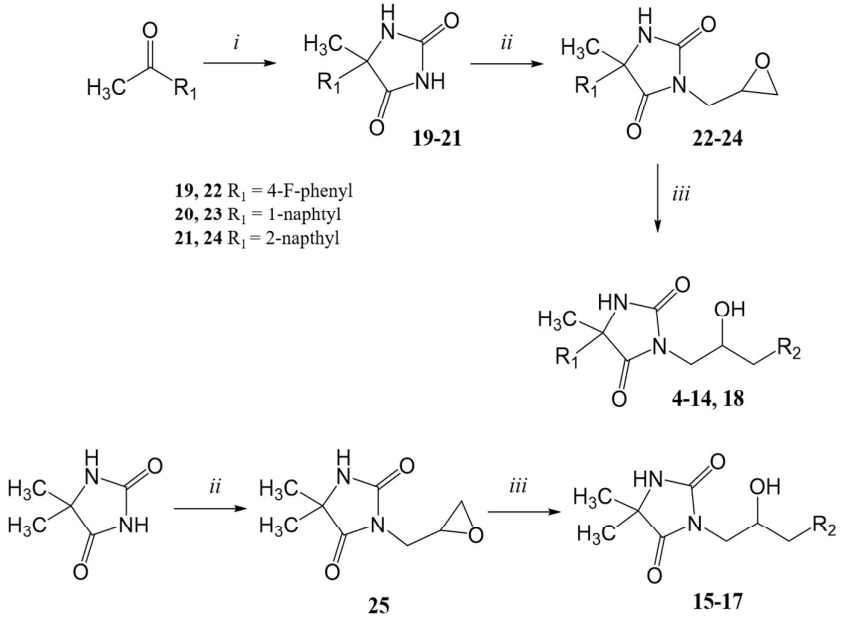

Scheme 1. Synthesis pathway for compounds **4–18**: (*i*) KCN, $(NH_4)_2CO_3$, 50% EtOH, 50°C, 24h; (*ii*) 2-(chloromethyl)oxirane, NaOH, H_2O, rt, 10h; (*iii*) R_2-commercially available derivative of piperazine/piperidine or isohexahydroquinoline, , solvent-free reaction, microwave irradiation 300-450W, 2 min.

X-ray crystallographic studies

The piperazine-hydantoin derivatives, obtained as modifications of lead **1**, were hard to give any crystal suitable for X-ray analysis, in particular, in the case of basic form that was also rare to precipitate during synthesis work up. Before, 5-phenyl-3-(3-(4-(2-ethoxyphenyl)piperazin-1-yl(-2-hydroxypropyl)-5-methylimidazolidine-2,4-dione hydrochloride was only one that gave a sufficient crystal for X-ray analysis, but in the salt form[19]. The present study has successfully provided the first representative crystal of basic form (compound **3**), appropriate for X-ray crystallographic analysis that allowed us to extend

View Article Online
DOI: 10.1039/C8MD00168E

knowledge about 3D-properties of this chemical group, which also supported molecular modeling.

The molecular geometry in the crystal structure of compound **3** with the atom numbering scheme is shown in Fig. 2.

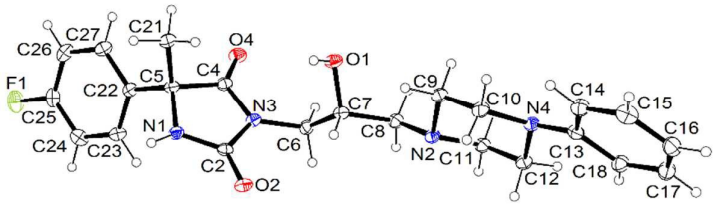

Fig. 2. The molecular structure of compound **3** showing the atom numbering scheme. Displacement ellipsoids are drawn at the 30% probability level.

The flexible aliphatic linker, which binds hydantoin and piperazine rings, shows an extended conformation, with the torsion angles being N3-C6-C7-C8 = 179.4(2)° and C6-C7-C8-N2 = 147.8(2)°. The bigger deviation of one value from 180° is due to the intramolecular contact C9-H9A···O1, for which the following parameters are observed: H9A···O1 = 2.59 Å, C9···O1 = 3.128(3) Å and the angle C9-H9A···O1 = 114°. The mutual orientation of 4-fluorophenyl substituent at C5 and hydantoin ring differs in comparison to geometry of the aforementioned (2-ethoxyphenyl)piperazine compound with phenyl ring at C5 atom, determined earlier [19]. The angle between the planes of the aromatic ring and the hydantoin ring is 62.2(1)°, while it is 86.73(5)° in the compared compound.

In the presented structure the piperazine ring adopts chair conformation, wherein the substituents at N2 and N4 are equatorial. The torsion angles C14-C13-N4-C10 and C18-C13-N4-C10 are 25.7(3)° and -157.3(3)°, respectively, which indicate that the phenyl ring at N4 atom is almost coplanar with piperazine moiety. The angle between the planes of aromatic and piperazine (C9, C10, C11, C12) rings is 10.3(2)°. We observed a higher value of the corresponding angle of 26.8(2)° for another hydantoin derivative with N-phenylpiperazine moiety[22].

The main intermolecular interactions are based on O-H···O and N-H···N hydrogen bonds (Fig. 3). One oxygen atom (O2) of hydantoin is involved in hydrogen bond with hydroxyl group, whereas the second oxygen atom (O4) is involved in C-H···O intermolecular interactions. The nitrogen atom (N1) of hydantoin is engaged in hydrogen bond with

View Article Online
DOI: 10.1039/C8MD00168E

nitrogen atom (N2) of piperazine ring. Furthermore, the fluorine atom makes C-H···F contacts. The parameters of these interactions are listed in Table 2.

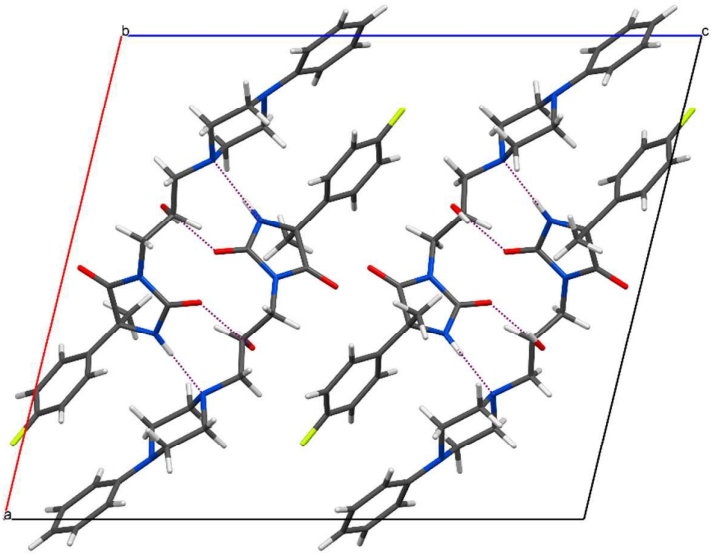

Fig. 3. Packing of molecules in the unit cell projected along [010] direction. Dashed lines indicate hydrogen bonds.

Table 2. The parameters of intermolecular interactions in structure **3**.

D-H···A	H···A (Å)	D···A (Å)	D-H-A (°)	Symmetry code
N1-H1N···N2	2.08(4)	2.981(3)	170(3)	-x+1, y-1/2, -z-1/2
O1-H1···O2	1.90(4)	2.756(3)	167(4)	-x+1, y-1/2, -z-1/2
C8-H8B···F1	2.61	3.319(3)	128.6	-x+1, -y+1, -z
C11-H11A···F1	2.77	3.464(3)	127.6	-x+1, -y+1, -z
C21-H21B···O4	2.36	3.334(3)	169.9	-x+1, -y, -z
C26-H26···O1	2.81	3.498(4)	130.3	-x+1, -y, -z
C27-H27···O4	2.50	3.368(4)	152.4	-x+1, -y, -z

Radioligand binding assays

The radioligand competition binding assays were applied to determine the affinity and selectivity profiles of the newly synthesized compounds (**4**–**18**) for human serotonin 5-HT_{7b}R, 5-HT_{1A}R, and dopaminergic D_{2L}R, stably expressed in HEK-293 cells (Table 1). Five compounds

View Article Online
DOI: 10.1039/C8MD00168E

from the series (**7**, **10**, **11**, **13**, **14**) were highly active toward 5-HT_7R (3 nM ≤ K_i ≤ 19 nM), whereas other five (**8**, **9**, **12**, **15**, **16**) demonstrated rather moderate activity (125 nM ≤ K_i ≤ 224 nM). Moreover, almost all the most active 5-HT_7R agents (**8–16**), excluding compound **7**, showed selectivity over 5-HT_{1A}R and D_2R. The active compound **7** had also potent affinity toward 5-HT_{1A}R (K_i = 19 nM).

ADME-Tox studies in vitro

The preliminary *in vitro* studies on ADME-Tox parameters were performed for selected, most active 5-HT_7R ligands (**7**, **10** and **13**) in comparison to the results for both leads (**1** and **2**) and the metabolically stable drug, aripiprazole. For this purpose, mouse liver microsomes (MLMs) and human embryonic kidney (HEK-293) or *hepatoma* (HepG2) cell lines were used according to the described previously protocols[20,21].

Metabolic stability

The incubation of the 5-HT_7R ligands (**2**, **7**, **10** and **13**) in the presence of MLMs followed by the UPLC-MS analyses, including ion fragmentation and supported by *in silico* simulation with MetaSite software, allowed to determine the metabolic stability, metabolic pathways and the most probable structures of the 5-HT_7R ligands' metabolites (details in Supplementary materials: Table S3, Fig. S1-S12).

Regarding the metabolic stability, the new compounds (**7**, **10** and **13**) were less stable than arirpiprazole (Table S3, Fig.S1-S9 v. Fig.S10, Supplementary materials). It was seen that ~65-70% of compounds **7** and **13** were metabolized into four or six metabolites, respectively, whereas ~40% of compound **10** into four metabolites. However, the metabolic stability of **10** was the closest to the most stable lead **2** (~20% remaining, Table 3) that metabolized into one metabolite (Table S3, Fig.S11 and S12, Supplementary).

Furthermore, the metabolic stability of the lead **2** and compounds **7**, **10** and **13** were determined in pharmacokinetic *in vitro* studies, performed by using MLMs in order to calculate the half-life period ($t_{1/2}$) and hepatic metabolic clearance CL_{int} and compared to the obtained previously data for the reference aripiprazole and the 1st generation lead **1**[20] (Table 3).

A comparison of the pharmacokinetic values ($t_{1/2}$, CL_{int}) for both leads (**1**[20] and **2)** has shown their similar metabolic stability in MLMs. In contrast, the new synthesized derivatives

View Article Online
DOI: 10.1039/C8MD00168E

(**7**, **10** and **13**) were less stable than both leads (**1** and **2**) and the reference aripiprazole but they demonstrated rather satisfying values of both $t_{1/2}$ and CL_{int}. The CL_{int} value of the most stable compound **10** was only ~1.7 fold higher than CL_{int} of the leads (**1** and **2**) and ~2.3 fold higher than that of metabolically stable aripiprazole, whereas the CL_{int} of the most labile compound **7** was ~3.5 fold higher than that of both leads and almost 5 fold higher in comparison to the value of aripiprazole (Table 3).

Table 3. Pharmacokinetic properties of the 5-HT_7R ligands and the reference drug aripiprazole estimated *in vitro* by MLMs

	Aripiprazole	**1***	**2**	**7**	**10**	**13**
$t_{1/2}$ (min)	217.0*	157.5*	157.5	45.0	94.0	62.5
mouse CL_{int} (ml/min/kg)	12.5*	17.2*	17.2	60.3	29.0	43.4
% of remaining substrate after 120 min of incubation	ND**	ND**	~20	~65	~40	~70

* values in MLMs estimated previously[20]; ** ND = no determined

Toxicity

Compounds **7**, **10** and **13** were tested for their safety in HEK-293 and HepG2 cell lines, at four concentration intervals (0.1–100 µM) for 72 h. The antiproliferative drug doxorubicin (DX) was used as a positive control at 1 µM. Additionally, the mitochondrial toxin carbonyl cyanide 3-chlorophenylhydrazone (CCCP), was used at 10 µM for assays with HepG2 (Fig. 4).

View Article Online
DOI: 10.1039/C8MD00168E

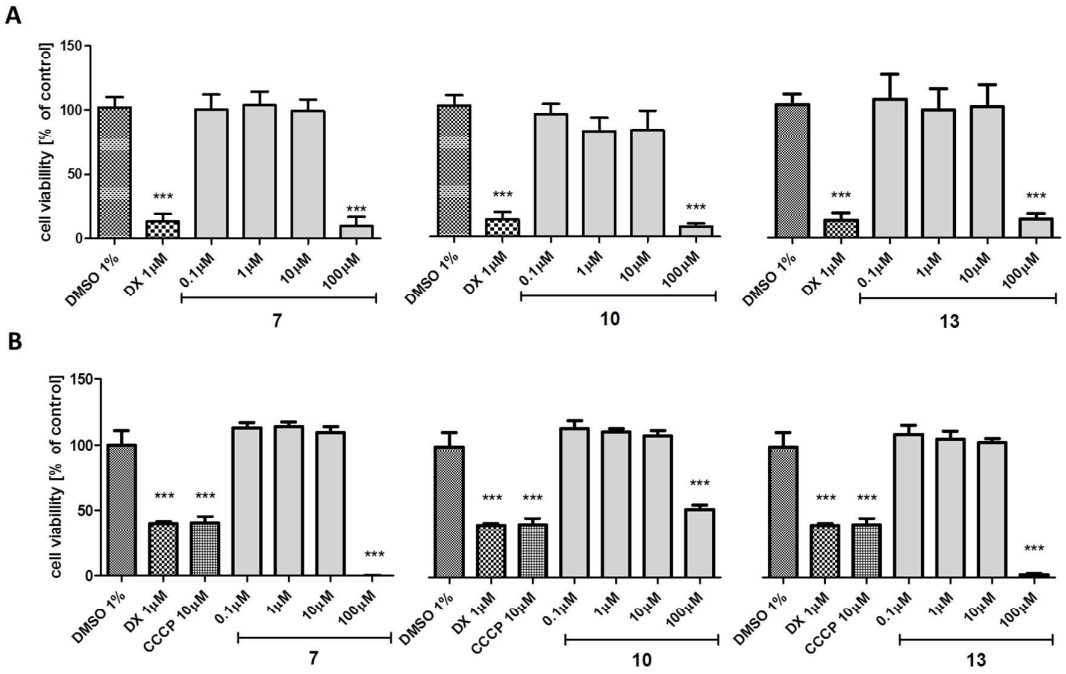

Fig. 4. The effect of **7** , **10** , **13** and doxorubicin (DX) on HEK-293 viability after 72h of incubation (A) . The effect of **7** , **10** , **13**, doxorubicin (DX) and carbonyl cyanide 3-chlorophenylhydrazone (CCCP) on HepG2 viability after 72h of incubation (B) The statistical significance was evaluated by a one-way ANOVA, followed by Bonferroni's Comparison Test (***p < 0.001 compared with negative control).

All examined compounds significantly influenced both cell lines viability, but only at the highest used dose (100 μM). However, the comparison of the obtained results to the effect of DX at the 1 μM or CCCP at 10 μM indicated rather weak cytotoxic and hepatotoxic effects of the examined 5-HT_7R ligands (Fig. 4). Regarding described previously effects of leads **1** and **2** on HEK-293 cells viability[20,21], compounds **7**, **10** and **13** were in the range of toxicity of the lead **2**.

Molecular modeling and SAR analysis

To support the discussion about aromatic ring localization and its influence on affinity towards 5-HT_7R, appropriate interfeature distances have been measured and compared with the known pharmacophore model requirements[23]. Moreover, all the compounds (**1–18**) were docked to homology models of 5-HT_7R in order to define key protein–ligand interactions. Additionally, due to the occurred 5-HT_7/5-HT_{1A} dual action for compound **7**, the docking studies to 5-HT_{1A}R homology models have been applied, as well.

View Article Online
DOI: 10.1039/C8MD00168E

Previously, we confirmed[19] that analogs of lead structure MF-8 (**1**) fit very well to the pharmacophore model of 5-HT$_7$R antagonists reported by Lopez-Rodriguez[23]. For this model, the optimal distance between basic center (N2) and hydrophobic (aromatic) area (ring centroid) is 5.4–6.4 Å, thus the arylpiperazine moiety met perfectly this requirement (Fig. 5A). The radioligand binding results showed significant relationship between N2–ring centroid distance and 5-HT$_7$R affinities of compounds **2–8** and **18**. Both, an increase and a decrease of this distance, beyond the optimum range, resulted in a significant reduction of 5-HT$_7$R affinity, e.g. compound **4** (Fig. 5B) and **6** (Fig. 5C), with N2-ring centroid distance > 6.4 Å, showed K_i = 2085 nM and 2172 nM, respectively, while compound **18** (Fig. 5D) with N2-ring centroid distance < 5.4 Å was also less active (K_i = 888 nM). Intriguing results were observed for the diphenylmethyl-containing lead **2** (K_i = 79 nM, Fig. 5E) if comparing to the inactive benzyl compound (**4**, Fig.5B). The presence of an additional aromatic ring changed geometry in the way that one of the phenyl group was closer to the basic center (6.30 Å), resulting with a significant 5-HT$_7$R activity improvement. Moreover, not only the presence of additional phenyl ring was profitable, but also the distance between this two phenyl rings (e.g. compound **2** *vs* **6**). Fused rings, as is observed in naphthalene moiety, linked to piperazine *via* methylene group (**6**, Fig. 5C), brought strong decrease of the 5-HT$_7$R affinity, whereas an introduction of diphenylmethyl group (**2**, **12**, and **17**) improved the 5-HT$_7$R affinity.

On the other hand, the naphthyl group linked directly to piperazine (**7**, Fig. 5F) provided very high affinity (K_i = 11 nM) and additionally, this structure turned out to be the first dual 5-HT$_7$/5-HT$_{1A}$ ligand coming from the herein- and previously described series[18,19].

View Article Online
DOI: 10.1039/C8MD00168E

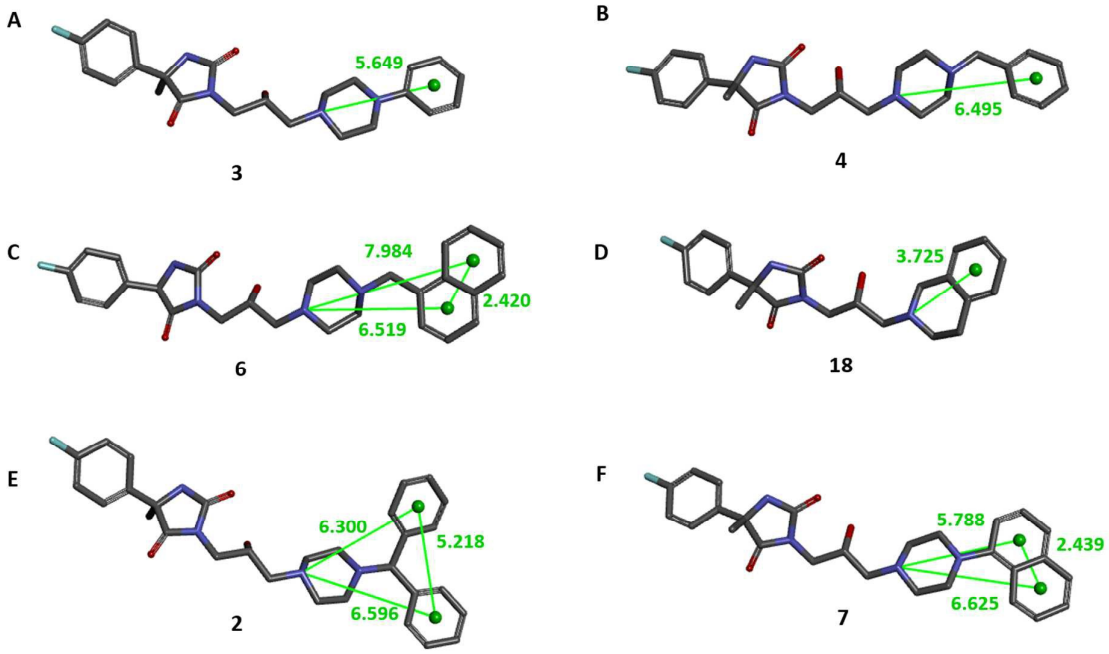

Fig. 5**.** Comparison of distances between basic center (N2) and aromatic centroids (presented as green lines and expressed in [Å]) for compounds **2**–**4**, **6**,**7** and **18**.

An analysis of the binding modes for compounds **4**, **6**, **7** and **18** (Fig. 6A) showed the influence of above-discussed distances on the receptor–ligand interactions. Although all compounds (**4**, **6**, **7** and **18**) interact with aromatic cluster formed by Phe6.51 and Phe6.52, the significant decrease of activity for compounds **4**, **6**, and **18** seems the be a consequence of loss of the salt bridge with Asp3.32, the key interaction linked with high 5-HT_7R affinity that is maintained only for the most active one (**7**).

Recently, we also indicated that introduction of additional phenyl ring into position 5 of hydantoin caused significant decrease of 5-HT_7R affinity[19]. Additionally, an exchange of phenyl into methyl group (resulting with 5,5-dimethylhydantoin moiety) led to decrease of 5-HT_7R activity (K_i = 125 nM for **15** vs K_i = 3 nM for the 1st generation lead **1**), but not so strong as in the case of presence of two phenyl rings (5,5-diphenylhydantoin, 189-fold decrease in respect to **1**)[19]. Interestingly, an exchange of the phenyl ring at position 5 of hydantoin into 1- or 2-naphthyl was profitable and did not disrupt the high 5-HT_7R affinity, making compounds **10**, **11**, **13** and **14** the most active ones in the whole series (**4**–**18**). For the naphthyl derivatives with the (2-methoxyphenyl)piperazine fragment (**10** and **13**), the 5-

View Article Online
DOI: 10.1039/C8MD00168E

HT_7R affinity was almost identical as that for the 1st generation lead **1**. No visible difference in 5-HT_7R affinity between compounds **10** and **13** seems to be a result of very well fitting of both aromatic moieties (1-naphthyl and 2-naphthyl) into the hydrophobic pocket formed by ECL2 and TM2, 3, and 7 (Fig. 6B). In comparison, an absence of the aromatic group in the case of compound **15** (with methyl group) influenced on lack of this additional stabilization, which resulted in decrease of activity. For the compounds with the (2-cyanophenyl)piperazine moiety (**11** and **14**), a little difference was visible, indicating that 2-naphtyl (**14**) was more preferable in respect to 1-naphthyl (**11**) group. The molecular docking of this pair of compounds (**11** and **14**), resulted in coherent binding mode to 5-HT_7R. However, there was a slight difference in hydantoin orientation, which might cause a weaker stabilization of this moiety by Arg7.36 (reported previously by our group[19]) for compound **11**, resulting in ~4-fold lower 5-HT_7R affinity than that for compound **14** (Fig. 6C).

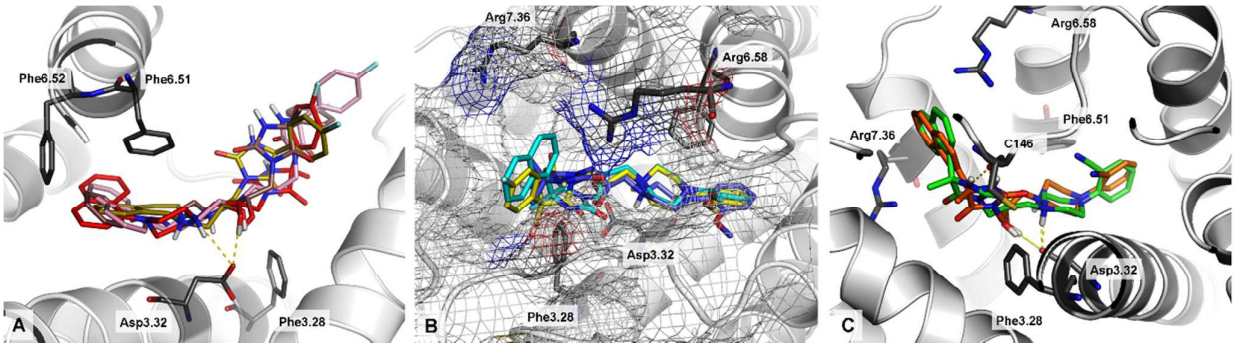

Fig. 6. (A) Influence of basic center-aromatic centroid distance on binding mode for compounds **4** (brown), **6** (pink), **7** (red) and **18** (olive); (B) The comparison of binding mode of lead structure, **1** (yellow) and its analogs with 2-naphthyl hydantoin moiety - **10** (cyan) and dimethylhydantoin - **15** (violet); (C) The comparison of binding mode of 1-naphthyl and 2-naphthyl hydantoin derivative with (2-cyanophenyl)piperazine moiety – **11** (orange) and **14** (green).

Worth mentioning that an introduction of the 1- and 2-naphthyl group, instead of the 4-fluorophenyl ring, allowed for keeping the 5-HT_7R selectivity over the 5-$HT_{1A}R$ and D_2R, however slightly less than that in the case of both, the 1st generation lead **1** (the highest 5-HT_7/D_2 selectivity ratio) and the 2nd generation lead **2** (the highest 5-HT_7/5-HT_{1A} selectivity ratio).

View Article Online
DOI: 10.1039/C8MD00168E

As the naphthylpiperazine derivative (**7**), the molecular docking to the 5-HT_{1A}R and 5-HT_7R homology models confirmed that structure **7** fit very well into the both binding pockets, and formed the following interactions: (i) a salt bridge with Asp3.32 and (ii) CH-π/π-π interaction between naphthyl group linked with piperazine and Phe6.52 side chain (Fig. 7). In comparison to the binding mode of dual ligands to 5-HT_{1A}R from different chemical class (2-benzoxazolones and 2-benzothiazolones) published previously[24], the compound **7** interacted also with Tyr7.43, while the hydrogen bond formation with Trp7.40 and Pro144 from EL2 was not observed. Regarding docking to the 5-HT_7R, the hydantoin moiety was hydrogen bonded by Arg7.43, similarly as the terminal heterocycle moiety of above-mentioned 2-benzoxazolones and 2-benzothiazolones derivatives.

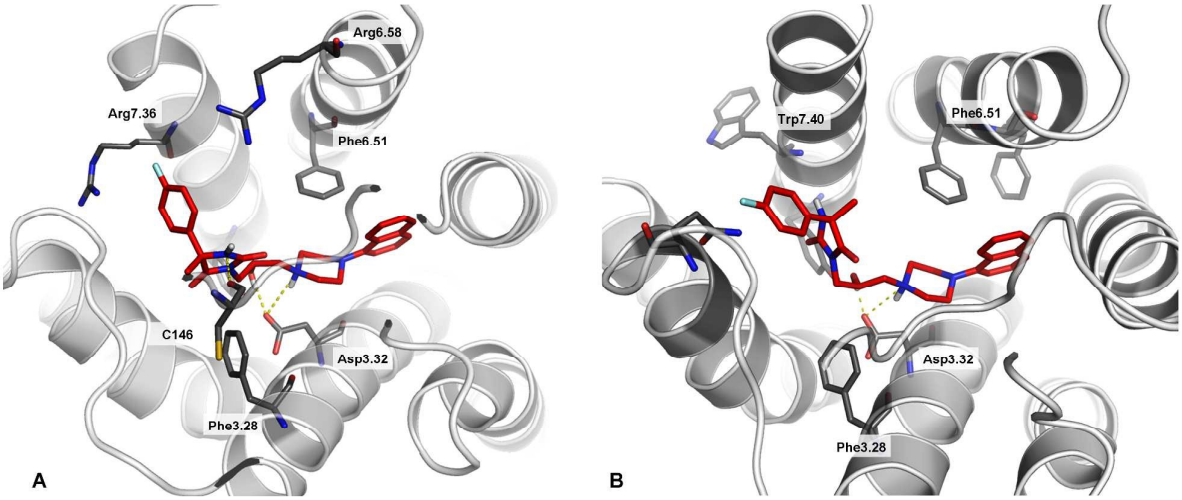

Fig. 7. Binding mode of compound **7** in 5-HT_7R (A) and 5-HT_{1A}R (B) homology models.

The size, type and spatial orientation of the aromatic rings influenced not only activity and selectivity but also metabolic stability properties of the investigated series (**1**-**18**). The lead **2**, with two unfused phenyl rings linked *via* methylene group to the piperazine and with mono-aromatic substituents at position 5 of hydantoin, has shown the high metabolic stability, predominantly in human[21], but also in mouse liver microsomes. In contrary, the presence of fused naphthyl rings either on the piperazine (**7**) or on hydantoin (**10**, **13**) sides resulted with some decrease of metabolic stabilities, especially distinct in the case of the β-naphthyl derivative (**13**). In contrary, an introduction of the naphthyl moiety, regardless of the

View Article Online
DOI: 10.1039/C8MD00168E

topology, did not significantly affect the safety, which was in the range of the lead 2 for all new derivatives (**7**, **10** and **13**).

Conclusions

Based on the 2nd generation lead (KKB16, **2**) and SAR analysis for the previous series, we have enriched the library of hydantoin-derived 5-HT_7R ligands by introducing 15 new members with diverse receptor affinities, especially potent in the case of 5-naphthylhydantoin derivatives. The performed X-ray analysis, molecular modeling and, consequently, comprehensive SAR-studies enabled to validate the role of changes in the number and (mutual) spatial orientation of aromatic rings for the 5-HT_7R activity and selectivity. We indicated that the 1- or 2-naphthyl moieties in position 5 of hydantoin were crucial feature for the potent action on 5-HT_7R with maintenance of distinct selectivity towards 5-HT_{1A}R and D_2R. In turn, the introduction of 1-naphthyl group on the piperazine side effected with significant 5-HT_7R and 5-HT_{1A}R dual action. The ADMET studies *in vitro*, performed for selected compounds (**7**, **10**, **13)** have confirmed their low cytotoxicity. The precise pharmacokinetic studies *in vitro* revealed in a general lower metabolic stability of naphthyl derivatives (**7**, **10**, **13)** in comparison to the leads (**1** and **2)** and aripiprazole, but more satisfying from "druglikeness" point of view for 1-naphthyl derivatives, especially, in the case of the naphthylpiperazine derivative (**7**). Bearing in mind these results, it would be worth to further investigate if both, the dual receptor action and lower (comparing with the leads) metabolic stability *in vitro,* are reflected in the pharmacological action *in vivo*, with special respect to antidepressant properties.

Material and methods

Synthesis

^{1}H NMR and ^{13}C NMR spectra were recorded on a Varian Mercury VX 300 MHz PFG instrument (Varian Inc., Palo Alto, CA, USA) in DMSO-d_6 at ambient temperature using the solvent signal as an internal standard. Data are reports using the following abbreviations: s, singlet; bs, broad singlet; d, doublet; t, triplet; m, multiplet; Ph, phenyl; Pp, piperazine, Ar,

View Article Online
DOI: 10.1039/C8MD00168E

aromatic, . Thin-layer chromatography was performed on pre-coated Merck silica gel 60 F_{254} aluminum sheets, the solvent systems used were methylene chloride/methanol 95:5. The mass for compounds **4-24** were recorded on a Waters ACQUITY^{TM} UPLC (Waters, Milford, MA, USA) coupled to a Waters TQD mass spectrometer (electrospray ionization mode ESI-tandem quadrupole). Retention times (t_R) are given in minutes. The UPLC/MS purity of all final compounds was determined (%). Syntheses under microwave irradiation were performed in a Samsung MW71B household microwave oven. The procedure for preparation of 5-methyl-5-naphthylhydantoins (**20**, **21**) and 5-(4-fluorophenyl)-5-methylhydantoin (**19**) and their spectral data has already been published[17,25,26]. Procedure for N-alkylation has been described before[19,27]. Physicochemical data for the oxirane **22** is available in the literature[27] and for oxiranes **23, 24** can be found in Supplementary.

General procedure for synthesis of final compounds (4-18)

5-(4-Fluorophenyl)-5-methyl-3-(oxiran-2-ylmethyl)imidazolidine-2,4-dione **17** (3.5 mmol, 1.0 eq) with appropriate piperazine derivative (3.0 mmol, 0.9 eq) in 50 mL flat-bottom flask were irradiated in household microwave: 450MW (2-3min). The progress of reaction was controlled by TLC (DCM/MeOH 95:5). The crude product was dissolved in methylene chloride. The resulted organic phase was washed with 2% HCl water solution, followed by water, then dried over Na_2SO_4, filtered through cotton and concentrated under vacuum to provide the desired product. Majority of the final products were transformed into hydrochloride salts by dissolving in 3-4 mL of 1.25 M HCl solution in ethanol. After 30 minutes of stirring at room temperature, resulted precipitates were filtered off, washed with 2-propanol and dried.

3-[3-(4-benzylpiperazin-1-yl)-2-hydroxypropyl]-5-(4-fluorophenyl)-5-methylimidazolidine-2,4-dione hydrochloride (4)

White solid. Yield 32%. LC/MS±: purity 98.05% t_R=3.69, (ESI) m/z [M+H] 441.29. 10.44 (s, 1H, NH^+), 9.01 (s, 1H, N^1H), 7.56-7.52 (m, 2H, Ar), 7.51-7.43 (m, 5H, Ar), 7.31-7.19 (m, 2H, Ar), 5.94 (s, 1H, CHOH), 4.23 (s, 1H, CHOH), 3.65-3.28 (m, 10H, N^3-CH_2, Ph-CH_2, Pp-2,6-H), 3.21-3.04 (s, 4H, Pp-CH_2, Pp-3,5-H), 1.72 (s, 3H, CH_3). ^{13}C NMR δ (ppm): ^{13}C NMR δ (ppm): 175.89, 169.58, 163.42, 160.99, 155.95, 155.86, 136.35, 136.32, 136.28, 135.19, 130.47, 128.98, 128.34, 128.27, 127.58, 115.81, 115.60, 62.95, 62.46, 59.35, 42.47, 25.95.

View Article Online
DOI: 10.1039/C8MD00168E

3-[3-(4-benzoylpiperazin-1-yl)-2-hydroxypropyl]-5-(4-fluorophenyl)-5-methylimidazolidine-2,4-dione hydrochloride (5)

White solid. Yield 29%. LC/MS±: purity 96.84% t_R=3.59, (ESI) m/z [M+H] 455.31. ^{1}H NMR δ (ppm): 10.54 (s, 1H, NH^+), 9.02 (s, 1H, N^1H), 7.56-7.53 (m, 2H, Ar), 7.37-7.12 (m, 7H, Ar), 5.98 (s, 1H, CHOH), 4.53 (m, 1H, CHOH), 4.35 (s, 2H, N^3-CH_2), 3.80-3.32 (m, 6H, Pp-3,5-H, Pp-CH_2), 3.30-2.92 (m, 4H, Pp-2,6-H), 1.72 (s, 3H, CH_3). ^{13}C NMR δ (ppm): 175.91, 175.87, 163.42, 160.99, 155.97, 155.89, 136.35, 128.94, 128.35, 128.27, 128.03, 127.03, 115.81, 115.59, 65.37, 63.42, 62.98, 62.95, 58.84, 58.73, 25.51, 15.63.

5-(4-fluorophenyl)-3-(2-hydroxy-3-{4-[(naphthalen-1-yl)methyl]piperazin-1-yl}propyl)-5-methylimidazolidine-2,4-dione (6)

White solid. Yield 43%. LC/MS±: purity 95.24% t_R=4.77, (ESI) m/z [M+H] 491.34. ^{1}H NMR δ (ppm): 9.02 (s, 1H, N^1H), 8.43 (s, 1H, Ar), 8.11-7.99 (m, 2H, Ar), 7.95 (s, 1H, Ar), 7.73-7.48 (m, 5H, Ar), 7.22 (t, *J* = 8.9, 2H, Ar), 4.88 (s, 2H, CH_2-Naphthyl), 4.26 (s, 1H, CHOH), 4.00-3.01 (m, 12H, Pp-2,3,5,6-H, Pp-CH_2, N_3-CH_2), 1.69 (s, 3H, CH_3). ^{13}C NMR δ (ppm): 175.90, 175.85, 163.40, 160.97, 155.97, 155.88, 136.38, 136.35, 136.33, 136.30, 133.90, 132.55, 130.80, 129.18, 128.36, 128.34, 128.28, 128.26, 127.47, 126.73, 125.82, 124.57, 115.80, 115.59, 62.96, 62.93, 42.43, 25.44.

5-(4-fluorophenyl)-3-{2-hydroxy-3-[4-(naphthalen-1-yl)piperazin-1-yl]propyl}-5-methylimidazolidine-2,4-dione hydrochloride (7)

White solid. Yield 36%. LC/MS±: purity 97.74% t_R=4.77, (ESI) m/z [M+H] 477.31. ^{1}H NMR δ (ppm): 10.82 (bs, 1H, NH^+), 9.07 (s, 1H, N^1H), 8.14-8.12 (d, *J* = 8.7 Hz, 1H, Ar), 7.96-7.87 (m, 1H, Ar), 7.67-7.65 (d, *J* = 8.2 Hz, 1H, Ar), 7.63-7.49 (m, 4H, Ar), 7.46-7.43 (t, *J* = 7.8 Hz, 1H, Ar), 7.24 (t, *J* = 7.6 Hz, 2H, Ar), 7.17-7.16 (d, *J* = 7.2 Hz, 1H, Ar), 6.00 (s, 1H, CHOH), 4.38 (s, 1H, CHOH), 3.82-3.13 (m, 12H, Pp-2,3,5,6-H, Pp-CH_2, N_3-CH_2), 1.75 (s, 3H, CH_3). ^{13}C NMR δ (ppm): 175.95, 175.90, 163.44, 161.01, 155.99, 155.91, 148.16, 136.40, 136.37, 136.33, 134.75, 128.86, 128.37, 128.31, 126.55, 126.40, 126.23, 124.46, 123.62, 115.83, 115.61, 115.52, 63.28, 62.99, 53.26, 42.62, 25.53.

5-(4-fluorophenyl)-3-[2-hydroxy-3-(4-phenoxypiperidin-1-yl)propyl]-5-methylimidazolidine-2,4-dione hydrochloride (8)

LC/MS±: purity 100.00% t_R=4.55, (ESI) m/z [M+H] 442.28. ^{1}H NMR δ (ppm): δ 10.56 (s, 1H, NH^+), 9.05 (s, 1H, N^1H), 7.62-7.50 (m, 2H, Ar), 7.30 (dd, *J* = 14.3, 7.4 Hz, 8H), 7.27 – 7.19 (m, 2H, Ar), 7.07-6.90 (m, 3H, Ar), 5.92 (s, 1H, CHOH), 4.74 (m, 1H, CH_aOH), 4.55 (m, CH_bOH, 1H), 4.29 (s, 1H, CH-O), 3.55-3.25 (m, 4H, N^3-CH_2, Pp-CH_2), 3.25-2.88 (m, 4H, Pp-2,6-H), 2.29-2.09 (m, 2H, Pp-3-H), 2.01-1.98 (m, 2H, Pp-5-H), 1.72 (s, 3H, CH_3). ^{13}C NMR δ (ppm): 175.86, 163.42, 160.99, 157.10, 156.79, 155.96, 136.36, 130.09, 128.35, 128.26, 121.68, 121.47, 116.73, 116.13, 115.81, 115.59, 70.53, 66.87, 63.43, 63.18, 63.09, 62.95, 59.54, 59.21, 51.61, 50.86, 48.75, 47.75, 47.63, 42.52, 26.56, 25.48.

View Article Online
DOI: 10.1039/C8MD00168E

3-{3-[4-(4-chlorophenoxy)piperidin-1-yl]-2-hydroxypropyl}-5-(4-fluorophenyl)-5-methylimidazolidine-2,4-dione hydrochloride (9)

White solid. Yield 58%. LC/MS±: purity 100.00% t_R=5.10, (ESI) m/z [M+H] 476.25 ^{1}H NMR δ (ppm): 10.55 (bs, 1H, N^+H), 9.04 (s, 1H, N^1H), 7.60-7.48 (m, 2H, Ar), 7.40-7.28 (m, 2H, Ar), 7.26-7.21 (m, 2H, Ar), 7.11-6.97 (m, 2H, Ar), 5.92 (s, 1H, CHOH), 4.74 (m, 1H, CH_aOH), 4.55 (m, CH_bOH, 1H), 4.28 (s, 1H, CH-O), 3.55-3.25 (m, 4H, N^3-CH_2, Pp-CH_2), 3.27-2.97 (m, 4H, Pp-2,6-H), 2.26-2.09 (m, 2H, Pp-3-H), 2.01-1.98 (m, 2H, Pp-5-H), 1.72 (s, 3H, CH_3). ^{13}C NMR δ (ppm): 175.86, 163.42, 160.99, 155.99, 155.96, 155.88, 155.67, 136.35, 129.86, 128.34, 128.26, 125.36, 125.13, 118.54, 117.90, 115.81, 115.59, 71.04, 67.44, 63.41, 63.17, 62.95, 59.49, 59.15, 51.57, 50.79, 48.67, 47.62, 42.52, 28.28, 28.20, 26.44, 25.95, 25.48.

3-{2-hydroxy-3-[4-(2-methoxyphenyl)piperazin-1-yl]propyl}-5-methyl-5-(naphthalen-1-yl)imidazolidine-2,4-dione (10)

White solid. Yield 48%. LC/MS±: purity 99.04% t_R=4.69, (ESI) m/z [M+H] 489.57. ^{1}H NMR δ (ppm): 8.79 (s, 1H, N^1H), 7.98-7.94 (m, 2H, Ar), 7.92-7.79 (m, 1H, Ar), 7.75-7.72 (d, *J* = 8.1 Hz, 1H, Ar), 7.60-7.44 (m, 3H, Ar), 6.98-6.78 (m, 4H, Ar), 4.92 (t, *J* = 5.2 Hz, 1H, CHOH), 4.16-3.99 (m, 1H, CHOH), 3.74 (s, 3H, OCH_3), 3.67-3.47 (m, 2H, N^3-CH_2), 2.94 (m, Pp-2,6-H, 4H), 2.57-2.49 (m, 4H, Pp-3,5-H), 2.40-2.39 (d, *J* = 5.9 Hz, 2H, Pp-CH_2), 1.92 (s, 3H, CH_3). ^{13}C NMR δ (ppm): 177.07, 156.58, 156.54, 152.39, 141.68, 134.46, 133.98, 133.93, 131.02, 130.93, 130.22, 129.63, 127.07, 126.10, 125.37, 124.50, 122.77, 121.26, 118.32, 112.28, 65.41, 65.21, 63.46, 63.39, 55.72, 54.07, 50.48, 26.72.

3-{2-hydroxy-3-[4-(2-cyanophenyl)piperazin-1-yl]propyl}-5-methyl-5-(naphthalen-1-yl)imidazolidine-2,4-dione hydrochloride (11)

White solid. Yield 44%. LC/MS±: purity 97.53% t_R=4.65, (ESI) m/z [M+H] 484.52. ^{1}H NMR δ (ppm) 10.93 (s, 1H, NH^+), 8.95 (s, 1H, N^1H), 8.95 (s, 1H, Ar), 7.99-7.95 (m, 2H, Ar), 7.88-7.70 (m, 3H, Ar), 7.68-7.45 (m, 4H, Ar), 7.27-7.07 (m, 2H, Ar), 6.05 (s, 1H, CHOH), 4.47 (s, 1H, CHOH), 3.82-3.49 (m, 6H, Pp-3,5-H; Pp-CH_2), 3.49-3.11 (m, 6H, N^3-CH_2, Pp-2,6-H), 1.98 (s, 3H, CH_3). ^{13}C NMR δ (ppm): 177.10, 177.06, 156.16, 154.20, 134.99, 134.74, 134.47, 133.77, 130.95, 130.90, 130.33, 129.73, 129.66, 127.25, 127.17, 126.94, 126.85, 126.14, 125.43, 124.55, 124.36, 123.48, 119.83, 118.37, 105.58, 63.69, 48.40, 26.62

3-{3-[4-(diphenylmethyl)piperazin-1-yl]-2-hydroxypropyl}-5-methyl-5-(naphthalen-1-yl)imidazolidine-2,4-dione hydrochloride (12)

White solid. Yield 33%. LC/MS±: purity 98.69% t_R=5.86, (ESI) m/z [M+H] 549.60 ^{1}H NMR δ (ppm): 10.57 (bs, 1H, NH^+), 8.94 (s, 1H, N^1H), 7.97 (m, 2H, Ar), 7.87-7.70 (m, 2H, Ar), 7.62-7.47 (m, 3H, Ar), 7.44-7.42 (d, *J* = 7.5 Hz, 4H, Ar), 7.33-7.23 (t, *J* = 7.4 Hz, 4H, Ar), 7.22-7.17 (m, 2H, Ar), 6.00 (s, 1H, CHOH), 4.43 (m, 2H, CHOH, Ph-CH-Ph), 3.63-3.40 (m, 4H, Pp-3,5-H), 3.20-3.13 (m, 4H, Pp-2,6-H), 2.79-2.77 (m, 2H, Pp-CH_2), 1.96 (s, 3H, CH_3). ^{13}C NMR δ (ppm): 177.07, 177.03, 156.15, 142.41, 134.47, 133.75, 130.95, 130.89, 130.33, 129.72, 129.65,

View Article Online
DOI: 10.1039/C8MD00168E

129.16, 129.02, 127.63, 127.18, 126.90, 126.12, 125.42, 124.46, 124.32, 74.17, 63.68, 52.63, 48.26, 42.33, 26.27.

3-{2-hydroxy-3-[4-(2-methoxyphenyl)piperazin-1-yl]propyl}-5-methyl-5-(naphthalen-2-yl)imidazolidine-2,4-dione hydrochloride (13)

White solid 42%. LC/MS±: purity 97.39% t_R=4.84, (ESI) m/z [M+H] 489.57. ^{1}H NMR δ (ppm): 10.63 (bs, 1H, NH^+), 9.11 (s, 1H, s, 1H, N^1H), 8.03 (s, 1H, Ar), 7.99-7.88 (m, 3H, Ar), 7.66-7.62 (m, 1H, Ar), 7.53-7.50 (m, 2H, Ar), 6.99-6.93 (m, 2H, Ar), 6.88-6.87 (m, 2H, Ar), 5.97 (s, 1H, CHOH), 4.33 (s, 1H, CHOH), 3.76 (s, 3H, OCH_3), 3.61 (s, 1H, CHOH), 3.55-3.39 (m, 6H, , Pp-3,5-H; Pp-CH_2), 3.21 (s, 2H, N_3-CH_2), 3.14-2.91 (m, 4H, Pp-2,6-H), 1.83 (s, 3H, CH_3). ^{13}C NMR δ (ppm): 175.97, 175.97, 156.08, 156.01, 156.01, 152.20, 139.84, 137.54, 137.49, 132.95, 132.76, 128.58, 127.84, 126.94, 124.83, 124.33, 123.82, 121.25, 118.58, 112.30, 63.51, 63.09, 55.78, 52.95, 47.17, 42.52, 24.98.

3-{2-hydroxy-3-[4-(2-cyanophenyl)piperazin-1-yl]propyl}-5-methyl-5-(naphthalen-2-yl)imidazolidine-2,4-dione hydrochloride (14)

White solid. Yield 38%. LC/MS±: purity 99.09% t_R=4.77, (ESI) m/z [M+H] 484.52.
^{1}H NMR δ (ppm): 10.82 (bs, 1H, NH^+), 9.10 (s, 1H, N^1H), 8.01 (s, 1H, Ar), 8.00-7.83 (m, 3H, Ar), 7.75-7.72 (t, *J* = 11.5 Hz, 1H), 7.65-7.60 (m, 2H, Ar), 7.53-7.50 (m, 2H, Ar), 7.22-7.12 (m, 2H, Ar), 5.98 (s, 1H, CHOH), 4.34 (s, 1H, CHOH), 3.51 (m, 6H, Pp-3,5-H; Pp-CH_2), 3.23 (m, 6H, N_3-CH_2; Pp-2,6-H), 1.81 (s, 3H, CH_3). ^{13}C NMR δ (ppm): 176.02, 156.09, 156.03, 154.18, 137.53, 137.48, 134.97, 134.73, 132.95, 132.76, 131.25, 128.67, 128.58, 127.84, 126.95, 124.87, 124.34, 123.45, 119.81, 118.36, 105.54, 63.51, 63.16, 59.05, 52.71, 48.37, 42.63, 24.97.

3-{2-hydroxy-3-[4-(2-methoxyphenyl)piperazin-1-yl]propyl}-5,5-dimethylimidazolidine-2,4-dione hydrochloride (15)

White solid. Yield 39%. LC/MS±: purity 98.25% t_R=3.04, (ESI) m/z [M+H] 377.28. ^{1}H NMR δ (ppm): 10.59 (s, 1H, NH^+), 8.37 (s, 1H, N^1H), 7.08-6.88 (m, 4H, Ar), 4.28-4.27 (m, 1H, CHOH), 3.79 (s, 3H, OCH_3), 3.66-3.63 (d, *J* = 11.6 Hz, 1H, CHOH), 3.52-3.40 (m, 4H, Pp-3,5-H), 3.42-3.05 (m, 8H, Pp-CH_2, N_3-CH_2, Pp-2,6-H), 1.30 (s, 6H, diCH_3).^{13}C NMR δ (ppm): 178.03, 155.70, 152.29, 139.66, 124.04, 121.30, 118.75, 112.45, 63.18, 59.30, 58.31, 55.85, 52.92, 51.64, 47.27, 47.15, 42.31, 25.04.

3-{2-hydroxy-3-[4-(2-cyanophenyl)piperazin-1-yl]propyl}-5,5-dimethylimidazolidine-2,4-dione hydrochloride (16)

White solid. Yield 51%. LC/MS±: purity 100.00% t_R=3.02, (ESI) m/z [M+H] 372.30. ^{1}H NMR δ (ppm): 10.93 (s, 1H, NH^+), 8.38 (s, 1H, N^1H), 7.76 (dd, *J* = 7.7, 1.5 Hz, 1H, Ar), 7.68-7.58 (m, 1H, Ar), 7.24 (d, *J* = 8.3 Hz, 1H, Ar), 7.18 (t, *J* = 7.5 Hz, 1H, Ar), 5.97 (s, 1H, CHOH), 4.30 (d, *J* = 7.0 Hz, 1H, CHOH), 3.75-3.59 (m, 4H, Pp-3,5-H), 3.45-3.10 (m, 8H, Pp-CH_2, N_3-CH_2, Pp-2,6-H), 1.32 (s, 6H, 2xCH_3). ^{13}C NMR δ (ppm): 178.02, 155.68, 154.21, 134.98, 134.74, 123.45, 119.83, 118.36, 105.57, 63.26, 59.32, 58.31, 52.68, 51.58, 48.42, 42.32, 25.04.

View Article Online
DOI: 10.1039/C8MD00168E

3-{3-[4-(diphenylmethyl)piperazin-1-yl]-2-hydroxypropyl}-5,5-dimethylimidazolidine-2,4-dione hydrochloride (17)

White solid. Yield 54%. LC/MS±: purity 100.00% t_R=4.64, (ESI) m/z [M+H] 437.30. ^{1}H NMR δ (ppm): 8.33 (s, 2H, N^{1}H), 7.40-7.32 (m, 10H), 4.21-4.18 (m, 2H, CHOH, Ph-CH-Ph), 3.49-2.96 (m, 12H, Pp-CH_2, N_3-CH_2, Pp-2,3,5,6-H), 1.31 (s, 6H, 2xCH_3).^{13}C NMR δ (ppm): 178.01, 155.69, 129.69, 128.66, 65.37, 63.47, 58.31, 42.23, 25.05, 25.03, 15.64.

5-(4-fluorophenyl)-3-[2-hydroxy-3-(1,2,3,4-tetrahydroisoquinolin-2-yl)propyl]-5-methylimidazolidine-2,4-dione (18)

White solid. Yield 42%. LC/MS±: purity 96.84% t_R=3.88, (ESI) m/z [M+H] 398.22 . ^{1}H NMR δ (ppm): 9.03 (bs, 1H, N^{1}H), 7.67 (s, 2H, Ar), 7.55-7.52 (m, 2H, Ar), 7.48-7.41 (m, 2H, Ar), 7.23 (td, *J* = 8.9, 1.0 Hz, 2H, Ar), 4.41-4.39 (m, 2H, N^3-CH_2), 4.26 (s, 1H, CHOH), 3.78-3.07 (m, 10H, Pp-CH_2, Pp-2,3,5,6-H), 1.70 (s, 3H, CH_3). ^{13}C NMR δ (ppm): 175.90, 175.85, 163.40, 160.97, 155.97, 155.88, 136.38, 136.35, 136.33, 136.30, 131.98, 130.04, 129.26, 128.36, 128.27, 115.81, 115.59, 63.39, 62.96, 62.93, 25.57, 25.44.

Crystallographic studies

The crystals of compound **3** suitable for X-ray structure analysis were obtained from a mixture of propan-2-ol and water solution by slow evaporation of the solvent at room temperature. The intensity data for single crystal were collected using the Oxford Diffraction SuperNova four circle diffractometer, equipped with the Mo (0.71069 Å) Kα radiation source and graphite monochromator. The phase problem was solved by direct methods using SIR-2014[28] and all non-hydrogen atoms were refined anisotropically using weighted full-matrix least-squares on F^2. Refinement and further calculations were carried out using SHELXL[29]. The hydrogen atoms bonded to carbons were included in the structure at idealized positions and were refined using a riding model with U_{iso}(H) fixed at 1.2 U_{eq} of C with the exception of hydrogen atoms in methyl group for which U_{iso}(H) fixed at 1.5 U_{eq}. Hydrogen atoms attached to nitrogen and oxygen atoms were found from the difference Fourier map and refined without any restraints. For molecular graphics ORTEP[30] and MERCURY[31] programs were used.

$C_{23}H_{27}FN_4O_3$, M_r = 426.48, crystal size = 0.39 x 0.13 x 0.02 mm^3, monoclinic, space group $P2_1/c$, a = 17.4230(7) Å, b = 6.0728(2) Å, c = 20. 2071(7) Å, V = 2077.9(1) Å^3, Z = 4, T = 130(2)K, 26816 reflections collected, 4984 unique reflections (R_{int} = 0.0787), R1 = 0.0738, wR2 = 0.1793 [I > 2σ(I)].

View Article Online
DOI: 10.1039/C8MD00168E

CCDC 1831620 contains the supplementary crystallographic data. These data can be obtained free of charge from The Cambridge Crystallographic Data Centre via www.ccdc.cam.ac.uk/data_request/cif.

Molecular modeling studies

Pharmacophore modeling

The 3-dimensional pharmacophore model was reconstructed by using the 3D QSAR Pharmacophore Generation protocol implemented in Discovery Studio 3.5. The structures of training compounds, as well as parameters were fetched from[23]. The conformation space of both training and synthetized compounds was generated using the BEST algorithm within a relative energy threshold of 20 kcal/mol above the global energy minimum and with a maximum number of generated conformations per ligand set to 255. The minimum distance between features was fixed at 2.5 Å, and the top 10 pharmacophore hypotheses were returned by the generation process and further used in the evaluation with reference pharmacophore model[23] with respect to the inter-feature distances and angles.

Molecular docking

The 3-dimensional structures of the ligands were prepared using LigPrep v3.6[32], and the appropriate ionization states at pH = 7.4 ± 1.0 were assigned using Epik v3.4[33]. Compounds with unknown absolute configuration were docked in R and S configurations. One low energy ring conformation per ligand was generated. The Protein Preparation Wizard was used to assign the bond orders, appropriate amino acid ionization states and to check for steric clashes. The receptor grid was generated (OPLS3 force field[34]) by centering the grid box with a size of 12 Å on Asp3.32 side chain. Automated flexible docking was performed using Glide v6.9 at SP level[35].

Radioligand binding assays

Affinities for human 5-HT_{1A}, 5-HT_{7b} and D_{2L} receptors

HEK-293 cells with stable expression of human 5-HT_{1A}, 5-HT_{7b} and D_{2L} receptors (prepared with the use of Lipofectamine 2000) were maintained at 37°C in a humidified atmosphere with 5% CO_2 and grown in Dulbecco's Modifier Eagle Medium containing 10% dialyzed fetal bovine serum and 500 µg/ml G418 sulfate. For membrane preparation, cells were subcultured in 150 cm^2 flasks, grown to 90% confluence, washed twice with phosphate

View Article Online
DOI: 10.1039/C8MD00168E

buffered saline (PBS) prewarmed to 37°C and pelleted by centrifugation (200 g) in PBS containing 0.1 mM EDTA and 1 mM dithiothreitol. Prior to membrane preparation, pellets were stored at −80°C.

Cell pellets were thawed and homogenized in 10 volumes of assay buffer using an Ultra Turrax tissue homogenizer and centrifuged twice at 35,000 × g for 15 min at 4°C, with incubation for 15 min at 37°C in-between. The composition of the assay buffers was as follows: for 5-HT_{1A}R: 50 mM Tris HCl, 0.1 mM EDTA, 4 mM $MgCl_2$, 10 µM pargyline and 0.1% ascorbate; for 5- HT_{7b}R: 50 mM Tris HCl, 4 mM $MgCl_2$, 10 µM pargyline and 0.1% ascorbate; for dopamine D_{2L}R: 50 mM Tris HCl, 1 mM EDTA, 4 mM $MgCl_2$, 120 mM NaCl, 5 mM KCl, 1.5 mM $CaCl_2$ and 0.1% ascorbate. All assays were incubated in a total volume of 200 µL in 96-well microtiter plates for 1 h at 37°C, except those for 5-HT_{1A}R which were incubated at room temperature. The process of equilibration was terminated by rapid filtration through Unifilter plates with a FilterMate Unifilter 96 Harvester (PerkinElmer). The radioactivity bound to the filters was quantified on a Microbeta TopCount instrument (PerkinElmer, USA). For competitive inhibition studies, the assay samples contained the following as radioligands (PerkinElmer, USA): 2.5 nM [^{3}H]-8-OH-DPAT (135.2 Ci/ mmol) for 5-HT_{1A}R; 0.8 nM [^{3}H]-5-CT (39.2 Ci/mmol) for 5-HT_7R or 2.5 nM [^{3}H]-raclopride (76.0 Ci/mmol) for D_{2L}R. Non-specific binding was defined with 10 µM of 5-HT in 5-HT_{1A}R and 5-HT_7R binding experiments, whereas 10 µM of haloperidol was used in D_{2L} assays. Each compound was tested in triplicate at 7 concentrations (10^{-10}–10^{-4} M). The inhibition constants (K_i) were calculated from the *Cheng-Prusoff* equation[36]. For all binding assays, results were expressed as means of at least two separate experiments (SD ≤ 19%).

ADME-Tox properties studies

The reference compound aripiprazole was synthesized and provided by Adamed Ltd. (Pieńków, Poland). The reference cytostatic drug doxorubicin (DX) and mitochondrial toxin carbonyl cyanide 3-chlorophenylhydrazone (CCCP)were provided by Sigma-Aldrich (St. Louis, MO, USA).

Mouse liver microsomes (MLMs): Microsomes from Liver, Pooled; biological source: from mouse *mus musculus* (CD-1), male; gene information: Mouse MGST-1 (56615) were purchased form Sigma-Aldrich (St. Louis, MO, USA).

View Article Online
DOI: 10.1039/C8MD00168E

The NADPH Regeneration System was purchased from Promega (Madison, WI, USA). All experiments were performed as described before[20,21].

Human embryonic kidney HEK-293 cell line ATCC CRL−1573 was kindly donated by Prof. Dr. Christa Müller (Pharmaceutical Institute, Pharmaceutical Chemistry I, University of Bonn). HepG2 (ATCC HB-8065) cell line was kindly donated by the Department of Pharmacological Screening, Jagiellonian University Medical College. The cell cultures' growth conditions were applied as described before[20,21]. The CellTiter 96® AQueous Non-Radioactive Cell Proliferation Assay (MTS) used for the cells' viability determination was purchased from Promega (Madison, WI, USA). The assays were performed as described previously[20,21]. The absorbance of the samples was measured using a microplate reader EnSpire (PerkinElmer, Waltham, MA USA) at 490 nm. GraphPad Prism™ software (version 5.01, San Diego, CA, USA) was used to calculate statistical significance.

Acknowledgements:

The authors would like to thank Prof. Dr. Christa Müller as well as to the research team of Department of Pharmacological Screening, Jagiellonian University Medical College for kind donating cell lines for the ADMET studies. The authors would like to thank Prof. Andrzej J. Bojarski for opportunity to carry out RBA studies in his Department and for all his helpful suggestions concerning this study. Described herein research was supported by National Science Center (Poland) Grant No. UMO-2014/15/N/NZ7/03072.

Conflict of Interest

The authors declare no competing interest.

References

1 M. Ruat, E. Traiffort, R. Leurs, J. Tardivel-Lacombe, J. Diaz, J. M. Arrang and J. C. Schwartz, *Proc Natl Acad Sci U S A*, 1993, **90**, 8547–8551.

2 S. B. Lovenberg TW1, Baron BM, de Lecea L, Miller JD, Prosser RA, Rea MA, Foye PE, Racke M, Slone AL, *Neuron*, 1993, **11**, 449–458.

3 J. A. Bard, J. Zgombick, N. Adham, P. Vaysse, T. A. Branchek and R. L. Weinshank, *J. Biol. Chem.*, 1993, **268**, 23422–23426.

4 A. Wesołowska, A. Nikiforuk, K. Stachowicz and E. Tatarczyńska, *Neuropharmacology*, 2006, **51**, 578–586.

5 A. Nikiforuk, T. Kos, K. Fijał, M. Hołuj, D. Rafa and P. Popik, *PLoS One*, 2013, **8**, e66695.

View Article Online
DOI: 10.1039/C8MD00168E

6 J. Śniecikowska, M. Głuch-lutwin, A. Bucki, P. Mierzejewski and M. Kołaczkowski, 2017, **26**, 165–178.
7 P. Bonaventure, C. Dugovic, M. Kramer, P. De Boer, J. Singh, S. Wilson, K. Bertelsen, J. Di, J. Shelton, L. Aluisio, L. Dvorak, I. Fraser, B. Lord, D. Nepomuceno, A. Ahnaou, W. Drinkenburg, W. Chai, C. Dvorak, S. Sands, N. Carruthers and T. W. Lovenberg, *J. Pharmacol. Exp. Ther.*, 2012, **342**, 429–440.
8 A. Zagórska, A. Bucki, M. Kołaczkowski, A. Siwek, M. Głuch-Lutwin, G. Starowicz, G. Kazek, A. Partyka, A. Wesołowska, K. Słoczyńska, E. Pękala and M. Pawłowski, *J. Enzyme Inhib. Med. Chem.*, 2016, **31**, 10–24.
9 A. Zagórska, M. Kołaczkowski, A. Bucki, A. Siwek, G. Kazek, G. Satała, A. J. Bojarski, A. Partyka, A. Wesołowska and M. Pawłowski, *Eur. J. Med. Chem.*, 2015, **97**, 142–154.
10 A. Anighoro, J. Bajorath and G. Rastelli, *J. Med. Chem.*, 2014, **57**, 7874–7887.
11 B. L. Roth, D. J. Sheffler and W. K. Kroeze, *Nat. Rev. Drug Discov.*, 2004, **3**, 353–359.
12 C. J. Suckling, J. A. Murphy, A. I. Khalaf, S. ze Zhou, D. E. Lizos, A. N. van Nhien, H. Yasumatsu, A. McVie, L. C. Young, C. McCraw, P. G. Waterman, B. J. Morris, J. A. Pratt and A. L. Harvey, *Bioorganic Med. Chem. Lett.*, 2007, **17**, 2649–2655.
13 M. J. Millan, *Neurotherapeutics*, 2009, **6**, 53–77.
14 B. Bang-Andersen, T. Ruhland, M. Jorgensen, G. Smith, K. Frederiksen and K. G. Jensen, *J. Med. Chem.*, 2011, **54**, 3206–21.
15 A. D'Agostino, C. D. English and J. A. Rey, *P T*, 2015, **40**, 36–40.
16 A. Loebel and L. Citrome, *BJPsych Bull.*, 2015, **39**, 237–241.
17 J. Handzlik, A. J. Bojarski, G. Satała, M. Kubacka, B. Sadek, A. Ashoor, A. Siwek, M. Więcek, K. Kucwaj, B. Filipek and K. Kieć-Kononowicz, *Eur. J. Med. Chem.*, 2014, **78**, 324–339.
18 K. Kucwaj-Brysz, D. Warszycki, S. Podlewska, J. Witek, K. Witek, A. G. Izquierdo, G. Satała, M. I. Loza, A. Lubelska, G. Latacz, A. J. Bojarski, M. Castro, K. Kieć-Kononowicz and J. Handzlik, *Eur. J. Med. Chem.*, , DOI:10.1016/j.ejmech.2016.02.024.
19 K. Kucwaj-Brysz, R. Kurczab, M. Jastrzębska-Więsek, E. Żesławska, G. Satała, W. Nitek, A. Partyka, A. Siwek, A. Jankowska, A. Wesołowska, K. Kieć-Kononowicz and J. Handzlik, *Eur. J. Med. Chem.*, , DOI:10.1016/j.ejmech.2018.01.093.
20 G. Latacz, A. Lubelska, M. Jastrzębska-Więsek, A. Partyka, K. Kucwaj-Brysz, A. Wesołowska, K. Kieć-Kononowicz and J. Handzlik, *Bioorg. Med. Chem. Lett.*, 2018, **28**, 878–883.
21 G. Latacz, A. Lubelska, M. Jastrzębska-Więsek, A. Partyka, A. Sobiło, A. Olejarz, K. Kucwaj-Brysz, G. Satała, A. J. Bojarski, A. Wesołowska, K. Kieć-Kononowicz and J. Handzlik, *Chem. Biol. Drug Des.*, , DOI:10.1111/cbdd.13106.
22 E. Żesławska, A. Kincses, G. Spengler, W. Nitek, K. Wyrzuc, K. Kieć-Kononowicz and J. Handzlik, *Bioorg. Med. Chem.*, 2016, **24**, 2815–2822.
23 M. L. López-Rodríguez, E. Porras, M. J. Morcillo, B. Benhamú, L. J. Soto, J. L. Lavandera, J. A. Ramos, M. Olivella, M. Campillo and L. Pardo, *J. Med. Chem.*, 2003, **46**, 5638–5650.
24 L. Salerno, V. Pittalà, M. N. Modica, M. A. Siracusa, S. Intagliata, A. Cagnotto, M. Salmona, R. Kurczab, A. J. Bojarski and G. Romeo, *Eur. J. Med. Chem.*, 2014, **85**, 716–726.
25 R. G. Murray, D. M. Whitehead, F. Le Strat and S. J. Conway, *Org. Biomol. Chem.*, 2008, **6**, 988.
26 J. Lee, J. Kim, J. S. Koh, H.-H. Chung and K.-H. Kim, *Bioorg. Med. Chem. Lett.*, 2006, **16**,

View Article Online
DOI: 10.1039/C8MD00168E

1954–1956.
27 R. Li, P. Hu, X. Ren, S. D. Worley and T. S. Huang, *Carbohydr. Polym.*, 2013, **92**, 534–539.
28 M. C. Burla, R. Caliandro, B. Carrozzini, G. L. Cascarano, C. Cuocci, C. Giacovazzo, M. Mallamo, A. Mazzone, G. Polidori and IUCr, *J. Appl. Crystallogr.*, 2015, **48**, 306–309.
29 G. M. Sheldrick, *Acta Crystallogr. Sect. C Struct. Chem.*, 2015, **71**, 3–8.
30 L. J. Farrugia and IUCr, *J. Appl. Crystallogr.*, 2012, **45**, 849–854.
31 C. F. Macrae, P. R. Edgington, P. McCabe, E. Pidcock, G. P. Shields, R. Taylor, M. Towler, J. van de Streek and IUCr, *J. Appl. Crystallogr.*, 2006, **39**, 453–457.
32 Schrödinger Release 2017-3: LigPrep, Schrödinger, LLC, New York, NY, 2017, (n.d.).
33 Schrödinger Release 2017-3: Epik, Schrödinger, LLC, New York, NY, 2017, (n.d.).
34 E. Harder, W. Damm, J. Maple, C. Wu, M. Reboul, J. Y. Xiang, L. Wang, D. Lupyan, M. K. Dahlgren, J. L. Knight, J. W. Kaus, D. S. Cerutti, G. Krilov, W. L. Jorgensen, R. Abel and R. A. Friesner, *J. Chem. Theory Comput.*, 2016, **12**, 281–296.
35 Schrödinger Release 2017-3: Glide, Schrödinger, LLC, New York, NY, 2017., (n.d.)
36 Y. Cheng and W. H. Prusoff, *Biochem. Pharmacol.*, 1973, **22**, 3099–108.

View Article Online
DOI: 10.1039/C8MD00168E

Table of contents information

Influence of presence and spatial orientation of aromatic ring(s) on 5-HT_7/5-HT_{1A} selectivity and activity were investigated within novel hydantoin-derived series.